2016 American Control Conference (ACC)
Boston Marriott Copley Place
July 6-8, 2016. Boston, MA, USA

Model-based Optimal Control of Layering Time for Layer-by-Layer UV Processing of Resin Infused Laminates

Adamu Yebi and Beshah Ayalew, *Member, IEEE*

***Abstract*— This paper first discusses experimental verifications of a 1D process model for layer-by-layer UV curing of thick composite laminates. The layer-by-layer UV curing process is modelled as a hybrid dynamic system by treating the underlying cure kinetics and associated thermal process as continuous dynamics switched by the discrete layering events. An additional heat transfer model is introduced to take into account the cooling effect of practical process delays of physically introducing each new layer. The successive layering times are treated as the control inputs that can be selected optimally via an optimization scheme that searches for the optimal layer addition times which result in minimal cure deviations across all layers of the laminate at final time. The potential benefit of the proposed optimal control scheme is demonstrated by considering both simulations and an experimental study on layer-by-layer fabrication of a thick composite laminate.**

Keywords: Layer-by-layer manufacturing, hybrid modeling of layer-by-layer manufacturing, control of UV curing process.

I. Introduction

Ultraviolet (UV) radiation technology is widely applied for curing of resin-infused materials due to its advantages of accelerated processing time, energy efficiency and favorable environmental impact[1, 2]. However, its application has largely been restricted to the curing of thin sections and coatings because of the limiting attenuation of UV radiation as it passes through thick target materials[3].

To overcome this attenuation challenge for thick sections, an approach of layer-by-layer deposition and curing is often adopted. Duan et al. [4] conducted an experiment that demonstrated the feasibility of the layer-by-layer curing approach for thick composite laminate fabrication. In another work, Wang[5] conducted model-based investigations of in-situ UV-laser curing of polymer composites using the filament winding method that aimed to cure relatively large thicknesses by applying the UV-laser on the tow while it is being wound on the mandrel. However, still some challenges remain that affect the product quality such as geometrical inaccuracy, material shrinkage, layer delamination, and residual stresses [6-10].

In our previous works[11-13], we proposed a stepped-concurrent layering and curing (SCC) process, where new layers are added before previous ones cure completely in such a way that the top of each layer is exposed to full UV intensity only part of the time so that cure level deviations and thermal stresses in the layers can be minimized. To further exploit the potential of the SCC approach, we then developed a systematic model-based dynamic optimization scheme by modeling the layering process as a hybrid dynamic system. In SCC, the successive addition of each layer changes both the spatial domains and the inter-layer conditions of the physical processes. This led us to the perspective that the process is a multi-mode hybrid system with a pre-defined mode sequence and a growing spatial domain. In[11], we motivated the need of optimal layer addition times for SCC and developed an optimization algorithm to compute this optimal layer addition times by treating them as the control inputs. Later in[12], we studied the effect of the augmented optimization of both layer-by-layer UV input intensity and inter-layer hold times as the control variables. More recently, we refined the optimization scheme considering robustness to model parameter uncertainties both with offline[13] and closed-loop configurations[14].

In all of the above previous works, the layering act is assumed to be instantaneous and the effect of practical process delays was neglected. However, significant effects were observed from such delays during our recent experimental study on the layer-by-layer UV curing of a composite laminate. The process delays between adding layers lead to a cooling effect that changes the dynamics of the distributed temperature in the layers. In the current paper, we build on the previous work, and address this limitation of the previous problem formulation. To this end, 1) we first discuss the process model validation for the layer-by-layer UV curing process using our recent experimental results; 2) then, we introduce an additional thermal model that captures the cooling effect due to practical layering delays; and 3) finally, we re-formulate the hybrid system model of the SCC using the experimentally validated process model and pursue model-based optimization for layering time control of the process. The main optimization objective in the SCC process is defined as a minimum overall cure level deviation at the final time. For this end-point optimization problem, we derive the first order optimality conditions directly by adjoining the coupled heat transfer dynamics (PDE) and cure kinetics dynamics (ODE) constraints of the layer-by-layer UV curing process model with the added process delay. The updated optimality conditions are briefly summarized (referring the reader to [13] for extended discussion on the derivation). These are then used to compute the optimal layer addition times. We illustrate the effectiveness of the proposed optimal control scheme by simulations and experiments on the layer-by-layer UV curing process for making a thick fiberglass composite.

* Research supported by NSF CAREER Grant CMMI-1055254.

A. Yebi is with the Clemson University International Center for Automotive Research, Greenville, SC 29607 (email: ayebi@clemson.edu).

B. Ayalew is with the Clemson University International Center for Automotive Research, 4 Research Dr, 342 CGEC, Greenville, SC 29607 (Corresponding author: phone 864-986-8690, email: ayebi@clemson.edu)

The remainder of the paper is organized as follows. Sections II gives a 1D model for a UV curing process, followed by some experimental verification of the extension of the model for layer-by-layer UV curing process, and the hybrid modelling re-formulation of the build-up process with practical process delay considerations. Section III provides the optimality conditions for the re-formulated model. Section IV offers demonstrative simulation and experimental results and discussions. Section V gives the conclusions of this contribution.

II. Problem Statement

A. 1D UV-curing Process Model

Consider the 1D UV curing process set up for a single laminate/layer shown in Fig. 1. The process model has three sub-models: 1) cure kinetics model that predicts the cure level evolution; 2) heat transfer model that accounts for heat generation due to exothermic reactions; and 3) a UV radiation attenuation model that accounts for the attention of UV intensity across the layer in the z-direction according to Beer Lambert's Law[15]. Other modeling considerations can be referred from[16]. The following coupled PDE-ODE system, along with the boundary and initial conditions, summarize the 1D process model for UV curing of a single layer:

$$\rho c_p \frac{\partial T(z,t)}{\partial t} = \frac{\partial}{\partial z}\left(k_z \frac{\partial T(z,t)}{\partial z}\right) + v_r \Delta H_r \rho_r \frac{d\alpha(z,t)}{dt} \quad (1a)$$

$$-k_z \frac{\partial T(0,t)}{\partial z} + \vartheta I_0 = h(T(0,t) - T_\infty) \quad (1b)$$

$$\frac{\partial T(l,t)}{\partial z} = 0 \quad (1c)$$

$$T(z,0) = T_0(z) \quad (1d)$$

$$\frac{d\alpha(z,t)}{dt} = s_0^q \exp(-\lambda p z)\, I_0^p K_D(\alpha)[K_1(T) + K_2(T)\alpha(z,t)]\left(1-\alpha(z,t)\right)\left(\bar{B} - \alpha(z,t)\right) \quad (1e)$$

$$K_D(\alpha) = \frac{1}{1+exp(\xi(\alpha(z,t)-\alpha_c))} \quad (1f)$$

$$K_1(T) = A_1 exp\left(\frac{-E_1}{RT_{abs}(z,t)}\right) \quad (1g)$$

$$K_2(T) = A_2 exp\left(\frac{-E_2}{RT_{abs}(z,t)}\right) \quad (1h)$$

$$\alpha(z,0) = \alpha_0(z) \quad (1i)$$

where ρ, c_p and k_z are the density, specific heat capacity and thermal conductivity of the composite laminate, respectively; $T(z,t)$ and $\alpha(z,t)$ are temperature and cure level distribution at depth z and time t, respectively; v_r, ρ_r and ΔH_r are volumetric fraction, density and polymerization enthalpy of resin in the composite matrix; ϑ is absorptivity constant of the UV radiation at the boundary; I_0 is UV input intensity at the surface; h is convective heat transfer at the top boundary; l is the thickness of a single layer, and T_∞ is constant ambient temperature; s_0 is photoinitiator concentration; p & q are constant exponents; λ is the absorption coefficient in the resin plus fiber; $\bar{B}$ is constant parameter related to reaction orders; ξ is diffusion constant; α_c is critical value of cure level; A_1 & A_2 are pre-exponential rate constants; E_1 & E_2 are activation energies; R is the universal gas constant; and $T_{abs}(z,t)$ is absolute temperature in Kelvin.

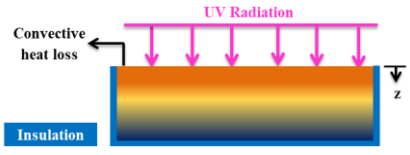

Figure 1: Schematic of a UV Curing Process

B. Experimental Model Verification

In our previous works[14, 16], we conducted three sets of experimental studies to identify the process parameters associated with the above 1D UV curing process model. These experimental studies included: 1) in-process UV transmission measurements to determine the UV attenuation constant λ; 2) cure kinetics studies by curing unsaturated polyester resin alone under controlled environment, to extract parameters related to the cure kinetics (A_1, A_2, E_1, E_2 & $\bar{B}$); and in-situ temperature measurements to determine process parameters related to heat convection and conduction. In[14], these experimental process parameter constants were identified for the UV curing process model (1a-1i) applied to fabricating a single layer of 5mm thick composite laminate.

In the current paper, we extend the experimental model verification for the layer-by-layer UV curing process. A schematic of experimental platform is given in Fig. 2. A UV LED (Clearstone42-cell, with nominal power of 16.1W) was used as the radiation source; an impresser (Barcol hardness according to ASTM D 2583) was used to quantify the through cure by measuring the hardness value at the top and the bottom of the cured laminate; and a DATAQ data logger was used to record the temperature measurement via T-type thermocouples. The insulation mold was made from polyisocyanurate foam, which was open at the top end to allow direct UV exposure on the laminate.

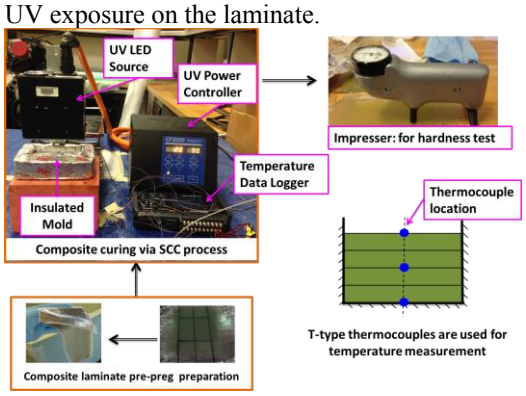

Figure 2: Experimental platform for fabricating thick composite laminate via SCC process

Using the experimental platform shown in Fig. 2, a 10mm thick composite laminate part with total of 10 layers was fabricated via a layer-by-layer process. Each layer ($\approx 1mm$ thick) is prepared via hand lay-up process that constitutes 3 fiber plies with volume ratio of 40% E-glass fiber and 60% of unsaturated polyester resin. A photoinitiator concentration of 0.1% by weight to that of resin was used. One layer was added at a time (by hand) and the cure was allowed to progress until the pre-optimized time for the addition of the next layer. A constant UV intensity of 100mW/cm^2 was used at each stage of layer addition. To validate the prediction capability of the process model, in-situ temperature measurement was recorded at interface at every second layer. The layer addition times were pre-optimized using the experimentally identified set of process parameters summarized in[14] for the 1D UV curing process model. These pre-optimized times were generated by neglecting process parameter uncertainties and process delay effects. In Fig. 3, the temperature measurement at every second layer interface is plotted along with the simulated temperature evolution. Interface-1 represents the node between the bottom-end layer and the layer immediately on

top of it and Interface-2 to Interface-8 are defined similarly as more layers are added. Note that the y-axis defines the direction of layer build up from bottom to top as shown in Fig. 4 below, while the z-axis depicts the direction of UV attenuation.

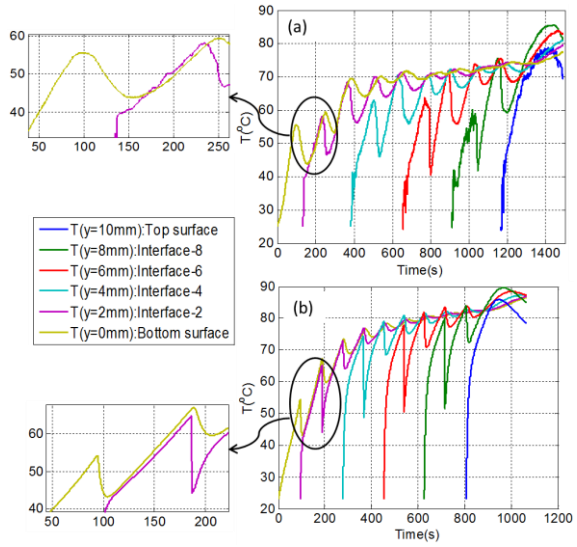

Figure 3: SCC process temperature evolution: (a) measured, and (b) simulated. (Overall time length for the simulated result is shorter than that of the measured one because the simulation neglected process delays).

The measured temperature in Fig. 3a, corroborates simulated predictions in Fig. 3b of the temperature cool down at the interface between layers due to the heat transfer between the pervious layer at the elevated temperature and newly added layer at ambient condition. However, some deviations are observed between the simulated and measured temperature that remained unexplained. These are attributed to sensor installation related noises in the measured temperature and additional heat loss/cooling effect/ due to practical process delays. The former is because the thermocouple installations were done by hand between layer build-ups in these experiments. For example, some corrupted measurements were recorded in some interfaces (e.g. Interface-8) until the thermocouple firmly settled in as the part cured. In addition to sensor related issues, the effect of practical process delays is observed in the measured data in terms of overall maximum temperatures achieved in all 10-layers. The highest possible temperature in the measured data is less than 85°C while the simulated temperature without delay considerations is about 90°C. Although this deviation between measured and simulated temperature may not seem too large for the considered experimental study on this low thermal conductivity polymeric material (10mm thick composite laminate with 10 layers), the consideration of process delay effects is important to include in the layer-by-layer hybrid process model to improve the general practicality and predictive ability of the hybrid model for optimization of the SCC layering times. To this end, the hybrid system model is re-formulated as discussed next.

C. Formulation of a Layer-by-Layer UV Curing Process as a Hybrid System with Process Delay

As mentioned above, for the layer-by-layer process, particularly for SCC, the successive addition of a new layer changes not only the spatial domain of the underlying cure kinetics and thermal processes, but also the heat transfer between the pervious layer at elevated temperature and the new layer at ambient conditions. This change can be captured by introducing modified initial conditions (IC) for the cure and temperature state at each layer addition, as well as updating the boundary conditions (BC) to reflect the increasing spatial domain as layers add on. One can view the layer addition event as switching the process dynamics from one mode (with given IC and BC) to another in a pre-defined switching sequence. Furthermore, since the layering is not quite an instantaneous switching as discussed above, we introduce an inter-mode process delay which is reflected in the continuous thermal dynamics of cooling just before the new layer addition. The re-formulated hybrid system view of the layer-by-layer curing process with inter-mode process delay is depicted schematically in Fig. 4.

In the following, a "mode-i" represents the number of i-layers subjected to the UV input and with continuous state dynamics evolution. The mode switching times are denoted by τ_i while $\delta\tau$ denotes a time delay before addition of new layer. The inter-modes shown by the dotted line in Fig.4 represent the spatial domain during the delay, which remains the same as that of the preceding mode.

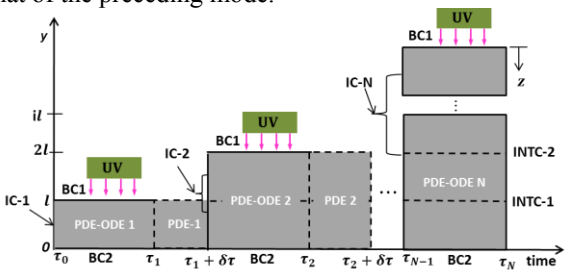

Figure 4: A hybrid system formulation of the layer-by-layer curing process with process delay

For this hybrid system view, the following assumptions and observations are considered: 1) the time delay is considered as a constant value for all layers assuming the layer-by-layer curing process (feasible for an automated operation). 2) The process delay/cooling effect/ is modeled by adding the PDE for thermal dynamics where the heat generation term from cure kinetics is neglected, assuming the UV power is turned off during the layer addition delay. 3) The switching/layering times are considered as the control variables that can be manipulated for a desired effect, in this case, for minimization of cure level deviations in a multi-layer part. Further details of this hybrid system realization of the layer-by-layer curing process, including additional assumptions and observations useful for extending the 1D UV curing process dynamics to the layer-by-layer manufacturing processes are given in our previous paper [12]. Here, we only summarize the mathematical description of the layer-by-layer process in the hybrid framework depicted in Fig. 4.

Denoting the thickness of the part after the i^{th} layer is added by il and introducing a coordinate transformation $y = il - z$ between the global y-axis and the local z-axis, and introducing notations $T_t^i(y,t), T_y^i(y,t), T_{yy}^i(y,t)$ and $\alpha_t^i(y,t)$ *for* $\partial T^i(y,t)/\partial t, \partial T^i(y,t)/\partial y, \partial^2 T^i(y,t)/\partial y^2$ and $\partial \alpha^i(y,t)/\partial t$, respectively, the state evolution for mode i in the time interval, $t \in [\tau_{i-1}, \tau_i]$ takes the form:

$$T_t^i(y,t) = aT_{yy}^i(y,t) + b(y)f^i\left(T^i(y,t), \alpha^i(y,t)\right) \quad on\ \Omega_\tau^i \quad (2a)$$

$$T_y^i(il,t) + eI_0 = c\left(T^i(il,t) - T_\infty\right) \quad on\ \Gamma_1^i \quad (2b)$$

$$T_y^i(0,t) = 0 \quad on\ \Gamma_2^i \quad (2c)$$

$$\alpha_t^i(y,t) = d(y) f^i\left(T^i(y,t), \alpha^i(y,t)\right) \quad on\ \Omega_\tau^i \quad (2d)$$

$$f^i\left(T^i(y,t), \alpha^i(y,t)\right) = I^p K_D^i(\alpha)\{K_1^i(T) + K_2^i(T)\alpha^i(y,t)\}\left(1 - \alpha^i(y,t)\right)\left(\bar{B} - \alpha^i(y,t)\right) \quad on\ \Omega_\tau^i \quad (2e)$$

where both the temperature state $T^i(y,t)$ and cure state $\alpha^i(y,t)$ evolve in the spatio-temporal domain defined by $\Omega_\tau^i = [0, il] \times [\tau_{i-1}, \tau_i]$. $0 \le \tau_0 < \tau_1 <, \cdots, < \tau_N < \infty$. The boundary conditions are also defined on $\Gamma_1^i = \{\text{il}\} \times [\tau_{i-1}, \tau_i]$, and $\Gamma_2^i = \{0\} \times [\tau_{i-1}, \tau_i$, $d(y) = s_0^q exp(-\lambda p(il - y))$, $b(y) = d(y)\left(v_r \Delta H_r \rho_r / \rho c_p\right)$, $a = k_z/\rho c_p$, $c = h/k_z$, and $e = \vartheta/k_z$; K_D, K_1 & K_2 are as given in (1f-1h). In the following analysis, for brevity, we use $f^i(T^i, \alpha^i)$ instead of $f^i\left(T^i(y,t), \alpha^i(y,t)\right)$, dropping the spatial and temporal indices of the state.

The state evolution of the delay dynamics for inter-mode i in the time interval, $t \in [\tau_i, \tau_i + \delta\tau]$, $i = 1,2,\cdots,N-1$ takes the form:

$$T_t^i(y,t) = aT_{yy}^i(y,t) \quad on\ \Omega_\tau^i \quad (3a)$$

$$T_y^i(il,t) + eI_0 = c\left(T^i(il,t) - T_\infty\right) \quad on\ \Gamma_1^i \quad (3b)$$

$$T_y^i(0,t) = 0 \quad on\ \Gamma_2^i \quad (3c)$$

For two or more layers, at the interface of new and earlier layers, the interface conditions (INTC) at $i = 1,2,\cdots,N-1$ are defined as:

$$\left[k_z T_y^i(il,t)\right]_{new\ layer} = \left[k_z T_y^i(il,t)\right]_{pervious\ layer} \quad (4a)$$

$$\left[T^i(il,t)\right]_{new\ layer} = \left[T^i(il,t)\right]_{pervious\ layer} \quad (4b)$$

At each switching time τ_i and $\tau_i + \delta\tau, i = 1,2,\cdots,N-1$, the transition to the new mode defines new initial conditions for the next mode. For the transition at τ_i, the initial conditions for state evolution of inter-mode i is described by:

$$T^i(y,\tau_i^+) = T^i(y,\tau_i^-) \quad (5)$$

For the transition at $\tau_i + \delta\tau$, the initial conditions for state evolution of mode $i+1$ is described compactly for both the temperature and cure state by:

$$T^{i+1}(y,\tau_i^+) = F^i\left(T^i(y,\tau_i^- + \delta\tau), T_0(y)\right) \quad (6a)$$

$$\alpha^{i+1}(y,\tau_i^+) = G^i\left(\alpha^i(y,\tau_i^-), \alpha_0(y)\right) \quad (6b)$$

where, $T^i(y,\tau_i^-)$ and $T^i(y,\tau_i^+)$ are the left hand and right hand limit values of the temperature state in mode i and inter-mode i, respectively, at the switching time τ_i, while $T^i(y,\tau_i^- + \delta\tau)$ and $T^{i+1}(y,\tau_i^+ + \delta\tau)$ defines the state at the switching time $\tau_i + \delta\tau$ in the inter-mode i and mode $i+1$, respectively $F^i: \Omega^i \to \Omega^{i+1}$ is the mode transition operator for the temperature state at switching time $\tau_i + \delta\tau$ defined over $\Omega^i \in [0, il]$. Since both states coexist in the spatial domain in all modes, similar definitions hold for the cure state (6b) as well, except that there is no cure evolution during the inter-mode delay.

For the simulation studies, a particular example of the mode transition operator of the form given in (7) below is considered, by assuming irreversibility of cure conversion for the cure state and average temperature at the interface of the new layer and the layer in the curing process. The initial value of all state elements corresponding to locations in the new layer are assumed to take on ambient conditions.

Temperature state mode transition operator:

$$F^i(T^i(y,\tau_i^- + \delta\tau), T_0(y)) = \begin{cases} T^i(y,\tau_i^- + \delta\tau),\ 0 \le y < il \\ \frac{1}{2}(T^i(y,\tau_i^- + \delta\tau) + T_0(y)), y = il \\ T_0(y),\ il < y \le (i+1)l \end{cases} \quad (7a)$$

Cure state mode transition operator:

$$G^i\left(\alpha^i(y,\tau_i^- + \delta\tau), \alpha_0(y)\right) = \begin{cases} \alpha^i(y,\tau_i^-), 0 \le y \le il \\ \alpha_0(y), il < y \le (i+1)l \end{cases} \quad (7b)$$

Equations (2-7) complete the hybrid formulation for the layer-by-layer UV curing process with inter-layer process delay consideration.

III. Optimal control of the Hybrid system

For the hybrid system described by (2-7), the optimal control problem can be posed as one of finding the optimal switching time vector $[\tau_1, \cdots, \tau_N]'$ that minimizes a cost function of the following form:

$$J(\tau_i, i = 1, \cdots, N) = \int_{\Omega^N} g\left(\chi^N(y,\tau_N^-)\right)dy + \sum_{i=1}^{N-1} \gamma^i(\tau_i^-) \quad (8)$$

where g is a terminal cost at final time τ_N , $\chi = [T, \alpha]'$ is augmented state of temperature and cure level, and $\gamma^i(\tau_i^-)$ is the cost associated with switching at τ_i. The initial time τ_0 and state $\chi(y,\tau_0)$ are assumed fixed, while the final time τ_N and state $\chi(y,\tau_N^-)$ are free to be optimized. To avoid confusion with the temperature state T, the transpose of a vector is denoted by $[\cdot]'$ instead of the usual $[\cdot]^{\mathrm{T}}$.

Optimality Conditions

In order to derive the necessary conditions for optimality, we first adjoin the dynamic constraint of the process dynamics (2) and (3), and transition constraints (4) to the cost function defined in (8) using Lagrange multipliers $\bar{p}^i(y,t)$ for the temperature state equation, $\bar{q}^i(y,t)$ for the cure level state equation, $\mu^i(y,\tau_i^-)$ for the temperature transition constraint, and $\eta^i(y,\tau_i^-)$ for the cure level transition constraint. The first-order necessary conditions for optimality are stated here. The derivation follows the one we detailed in[13]. Here, we only summarize the final optimality conditions. We neglect the switching cost.

Necessary conditions: An extremum to the cost defined in (8) with constraints (2-7) can be achieved by choosing a control variable $[\tau_1, \cdots, \tau_N]'$ that satisfies the following conditions:

a) For $t \in [\tau_{i-1}, \tau_i + \delta\tau]$, the following adjoint equations for process dynamics in mode i hold.

$$\bar{p}_t^i(y,t) = -a\bar{p}_{yy}^i(y,t) - \{b(y)\bar{p}^i(y,t) + d(y)\bar{q}^i(y,t)\} f_T^i\left(T^i, \alpha^i\right) \quad on\ \Omega_\tau^i \quad (9a)$$

$$\bar{p}_y^i(il,t) = c\bar{p}^i(il,t) \quad on\ \Gamma_1^i \quad (9b)$$

$$\bar{p}_y^i(0,t) = 0 \quad on\ \Gamma_2^i \quad (9c)$$

$$\bar{q}_t^i(y,t) = -\{b(y)\bar{p}^i(y,t) + d(y)\bar{q}^i(y,t)\} f_\alpha^i\left(T^i, \alpha^i\right) \quad on\ \Omega_\tau^i \quad (9d)$$

where $f_a^i\left(T^i, \alpha^i\right) = \partial f^i\left(T^i, \alpha^i\right)/\partial a$, for $a, b \in [T, \alpha]$.

b) For $t \in [\tau_i, \tau_i + \delta\tau]$, the following adjoint equations for process dynamics in inter-mode i hold.

$$\bar{p}_t^i(y,t) = -a\bar{p}_{yy}^i(y,t) \quad on\ \Omega_\tau^i \quad (10a)$$

$$\bar{p}_y^i(il,t) = c\bar{p}^i(il,t) \quad on\ \Gamma_1^i \quad (10b)$$

$$\bar{p}_y^i(0,t) = 0 \quad on\ \Gamma_2^i \quad (10c)$$

c) At $t = \tau_N$, the augmented adjoint variable vector $\Lambda(y,t) = \left[\bar{p}^i(y,t), \bar{q}^i(y,t)\right]'$ should satisfy:

$$\Lambda(y,\tau_N^-) = g_{\chi^N}(\chi^N(y,\tau_N^-)) \quad (11)$$

where, $g_{\chi^N}(\chi^N(y,\tau_N^-)) = \partial g(\chi^N(y,\tau_N^-))/\partial\chi^N$.

d) At any time $t = \tau_i + \delta\tau$, $i = i = 1,2,\cdots,N-1$, we have

$$\Lambda^{Ti}(y,\tau_i^- + \delta\tau) = F_T^{i\prime}\left(T^i(y,\tau_i^- + \delta\tau), T_0(y)\right)\Lambda^{Ti+1}(y,\tau_i^+ + \delta\tau) \quad (12a)$$

$$\Lambda^{\alpha i}(y,\tau_i^- + \delta\tau) = G_\alpha^{i\prime}\left(\alpha^i(y,\tau_i^- + \delta\tau), \alpha_0(y)\right)\Lambda^{\alpha i+1}(y,\tau_i^+ + \delta\tau) \quad (12b)$$

where $\Lambda^{Ti}(y,\tau_i^-) = \bar{p}^{Ti}(y,\tau_i^-)$, $\Lambda^{\alpha i}(y,\tau_i^-) = \bar{q}^{\alpha i}(y,\tau_i^-)$, $F_T^i = \partial F^i/\partial T^i$ *and* $G_\alpha^i = \partial G^i/\partial \alpha^i$.

e) At any time $t = \tau_i,\ i = i = 1,2,\cdots,N-1$, we have

$$\Lambda^{Ti}(y,\tau_i^-) = \Lambda^{Ti}(y,\tau_i^+) \quad (13a)$$

$$\Lambda^{\alpha i}(y,\tau_i^-) = \Lambda^{\alpha i}(y,\tau_i^- + \delta\tau) \quad (13b)$$

f) For switching time vector $\sigma_i = \tau_i + \delta\tau, i = 1,2,\cdots,N-1$, the optimality conditions in (13a) should hold, and for τ_N, (13b) should hold:

$$H^i(\sigma_i^-) - H^{i+1}(\sigma_i^+) = 0 \quad (14a)$$

$$H^N(\tau_N^-) = 0 \quad (14b)$$

where, $\sigma_i^- = \tau_i^- + \delta\tau,\ \sigma_i^+ = \tau_i^+ + \delta\tau$; and

$$H^i(\sigma_i^-) = \int_{\Omega^i}\left[a\bar{p}^i(y,\sigma_i^-)T_{yy}^i(y,\sigma_i^-) + \{b(y)\bar{p}^i(y,\sigma_i^-) + d(y)\bar{q}^i(y,\sigma_i^-)\}f^i(T^i,\alpha^i)\right]dy \quad (15)$$

Note that the above summarized necessary optimality conditions return $\sigma_i, i = 1,2,\cdots,N-1$, and then the switching time τ_i is computed from $\tau_i = \sigma_i - \delta\tau$ for a given constant time delay $\delta\tau$. For this work, the steepest descent algorithm given in[11] with Armijo's step size[17] is used to compute the control variables σ_i & $\tau_N,\ i = 1,2,\cdots,N-1$.

IV. Results And Discussion

In this section, we present some results to demonstrate the feasibility of the proposed optimization scheme with practical process delay considerations using both simulation and experimental results for the fabrication of a thick composite laminate through the SCC process. Here, we are interested in achieving a through cure in all layers with minimum overall deviation at the end of the curing process by optimizing the inter-layer hold times. The desired optimization objective is described by selecting a nominal terminal cost function g in (8) of the form:

$$\bar{g}(\chi^N(y,\tau_N^-) = 0.5\{\alpha^N(y,\tau_N^-) - \alpha_d(y)\}^2, y \in [0, Nl] \quad (12)$$

For the process simulation and implementation of the optimization algorithm, a 10-node spatial discretization is adopted to convert the temperature state PDEs to a set of ODEs in time, for each layer. In the simulations, we used experimentally verified process parameters summarized in [14] for a fiberglass composite laminate with resin/fiber volume ratio of 60% /40%. The results are generated for a sample thickness of 10 mm with total number of 10 layers with an approximate thickness of 1mm per layer. A cure level of 90% was set as a desired final cure level across the part. A constant UV-intensity of 100 mW/cm^2 is used for curing mode and turned off during layer addition delay (inter-mode), which is assumed to be 10 sec for all layers.

We illustrate the advantages of the proposed optimization scheme by comparing the results of the following cases. Case 1: A non-optimal approach with equal-interval layering time and constant UV input; Case 2: An optimal approach with optimal layering time control and constant UV input. For the non-optimal approach (Case 1), the length of overall curing time is kept the same as that of the overall curing duration of the optimal approach (Case 2). For optimal case, the optimization is executed using the nominal model (no model uncertainties) until the desired performance is achieved. The comparisons of the two cases are given in Figs. 5 and 6 below.

Figure 5 shows that for the non-optimal case of equal-interval layering time, over cure is observed for the bottom layers while unacceptable cure level is achieved in the last few top layers compared to the desired cure level. The model-based optimization scheme offers near through cure in the final cure level distribution with overall cure level deviation of less than 6%. Figure 6 shows the trend of the optimal inter-layer hold times (layer addition times, including the delay). It first decreases form its value for the first few bottom most layers, seems to settle to a minimum for the middle layers before becoming highest in magnitude at the end as one adds layers from the bottom to the top. The longer hold times computed for the bottom most layers can be explained by a need to pre-compensate the anticipated large UV attenuation in the bottom layers as layers add on later. Similarly, the longer hold times for the top most layers can be explained by the need for bringing the cure level from zero to the desired 90% quickly while those at the bottom continue to cure with attenuated UV during this time.

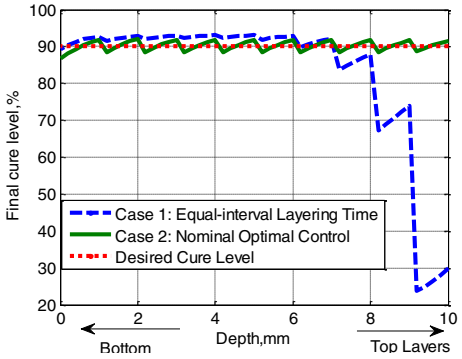

Figure 5: Achieved final cure level profile with optimal and equal-interval time control

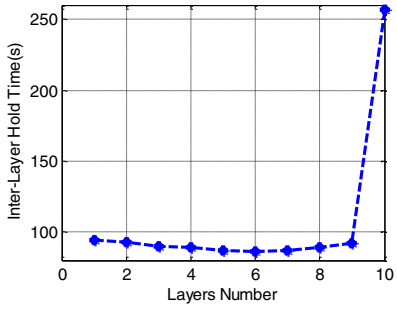

Figure 6: Optimized inter-layer hold (layering) times

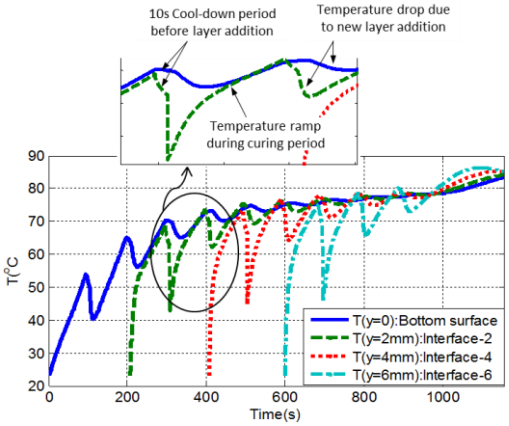

Figure 7: Temperature evolution at selected interfaces of layer addition

To show the curing temperature change due to process delay before new layer addition, the evolution of temperature at few selected interfaces is plotted in Fig. 7. The results show

further temperature drops (cooling effects) at the interfaces that eventually increase again as cure progresses with the added new layers.

Experimental study

To validate the advantage of model-based optimization of layering times, we applied the SCC process for curing three 10-layer samples by deviating the layer addition times from their optimized values. For the cured sample, through cure is verified by conducting hardness tests at the top and bottom surfaces. The comparative hardness test values and the applied layer addition times are summarized in Tables 1 and 2, respectively. Four different hardness values are measured for each sample, and an average value is considered for the analysis of the through-cure by comparing the values at the top and bottom surfaces. This average value is also compared to that of a reference sample of a thin section completely cured in one shot. The hardness test indentation points for each sample are shown in Figure 8.

Table 1: Hardness values fabricated parts (T-top & B-bottom)

	HARDNESS VALUE					REMARK
	1	2	3	4	AVG.	
Sample #1	48	50	46	45	47T	With 20 sec deviation from each optimal layering time
	32	35	33	38	35B	
Sample #2	49	51	48	49	49T	With 10 sec deviation from each optimal layering time
	39	37	41	40	39B	
Sample #3	51	49	52	53	51T	With optimal layering time
	45	46	45	44	45B	
Reference sample	55	56	54	54	55T	
	52	54	53	54	53B	

Table 2: Layer addition times (layers numbered from bottom to top)

	Layer #									
	1	2	3	4	5	6	7	8	9	10
Sample #1	75	74	72	71	69	69	70	71	74	240
Sample #2	85	84	82	81	79	79	80	81	84	250
Sample #3	95	94	92	91	89	89	90	91	94	260

As summarized in Table 1, relatively large hardness values are measured for sample #3 with optimal layering times, while the other two sample cases result lower hardness values. This is supported by fine indentation points shown for sample #3 in Fig. 8 as compared to the other two cases. In addition, for sample #3, a hardness value of over 88% is measured as compared to that of top surface, and 85% to that of the reference sample. These experimental results illustrate the feasibility and benefits of curing thick parts via model-optimized SCC process to alleviate the effects from UV attenuation.

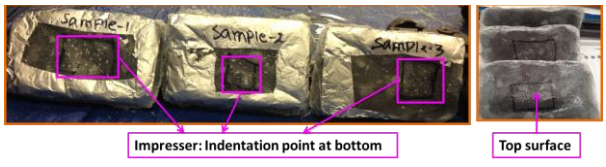

Figure 8: Hardness indentations on samples cured via SCC process

V. CONCLUSIONS

The paper first offered discussions on experimental model verifications of a proposed layer-by-layer curing process of fabricating thick resin-infused polymer composite laminates. Therein, justifications have been given for adding inter-layer process delays in the hybrid system modeling of the layer-by-layer UV curing process. The delays introduce an inter-mode that affects the thermal dynamics of the process. Then, the paper offered an optimization scheme by adjoining the modified hybrid dynamics model of the layer-by-layer process to determine the optimal layer addition times. The paper included both simulation and experimental results that illustrated the benefit of the proposed process to fabricate a thick layer despite the UV attenuation in the part. The results illustrated the advantages of the optimization via the hybrid model in achieving near-through cure with minimal final cure level deviation.

REFERENCES

[1] P. Roose;, I. Fallais;, C. Vandermiers;, M. G. O. ;, and M. Poelman, "Radiation curing technology: An attractive technology for metal coating," *Progress in Organic Coatings* vol. 64, pp. 163-170, 2009.

[2] P. Compston, J. Schiemer, and A. Cvetanovska, "Mechanical properties and styrene emission levels of a UV-cured glass-fibre/vinylester composite," *Composite Structures,* vol. 86, pp. 22-26, 2008.

[3] A. Endruweit, M. S. Johnson, and A. C. Long, "Curing of composite components by ultraviolet radiation: A review," *Polymer composites,* vol. 27, pp. 119-128, 2006.

[4] Y. Duan, J. Li, W. Zhong, R. G. Maguire, G. Zhao, H. Xie, *et al.*, "Effects of compaction and UV exposure on performance of acrylate/glass-fiber composites cured layer by layer," *Journal of Applied Polymer Science,* vol. 123, pp. 3799-3805, 2012.

[5] X. Wang, "Modeling of in-situ laser curing of thermoset-matrix composites in filament winding," PhD Dissertation, University of Nebraska, 2001.

[6] G. Tapia and A. Elwany, "A Review on Process Monitoring and Control in Metal-Based Additive Manufacturing," *Journal of Manufacturing Science and Engineering,* vol. 136, 2014.

[7] N. Guo and M. C. Leu, "Additive manufacturing: technology, applications and research needs," *Frontiers of Mechanical Engineering,* vol. 8, pp. 215-243, 2013.

[8] K. Zeng, D. Pal, and B. Stucker, "A review of thermal analysis methods in Laser Sintering and Selective Laser Melting," in *Proceedings of the Solid Freeform Fabrication Symposium*, Austin, TX, pp. 796-814, 2012.

[9] S. L. Campanelli, G. Cardano, R. Giannoccaro, A. D. Ludovico, and E. L. J. Bohez, "Statistical analysis of the stereolithographic process to improve the accuracy," *Computer-Aided Design,* vol. 39, pp. 80-86, 2007.

[10] K. Zeng, N. Patil, H. Gu, H. Gong, D. Pal, T. Starr, *et al.*, "Layer by Layer Validation of Geometrical Accuracy in Additive Manufacturing Processes," in *Proceedings of the Solid Freeform Fabrication Symposium*, Austin, TX, pp. 12-14, 2013.

[11] A. Yebi and B. Ayalew, "Optimal Layering Time Control for Stepped-Concurrent Radiative Curing Process," *Journal of Manufacturing Science and Engineering,* vol. 137, p. 011020, 2015.

[12] A. Yebi and B. Ayalew, "A hybrid modeling and optimal control framework for layer-by-layer radiative processing of thick sections," in *American Control Conference (ACC),* , pp. 3619-3624, 2015.

[13] A. Yebi and B. Ayalew, "A Hybrid Modeling and Robust Optimal Control for Layer-by-Layer Manufacturing Process " *IEEE Transactions on Control Systems Technology (submitted, in review),* 2015.

[14] A. Yebi,.B. Ayallew, S. Pilla and X. Yu, "Model-based Robust Optimal Control for Layer-by-Layer UV Processing of Composite Laminates," *Journal of Dynamic Systems, Measurement, and Control (submitted, in review),* 2015.

[15] M. F. Perry and G. W. Young, "A mathematical model for photopolymerization from a stationary laser light source," *Macromolecular theory and simulations,* vol. 14, pp. 26-39, 2005.

[16] A. Yebi, B. Ayalew, and S. Pilla, "Control-Oriented Model Verification for UV Processing of Composite Laminate " in *Society for the Advancement of Material and Process Engineering (SAMPE),*, Baltmore,ML, May 19-21, 2015.

[17] L. Armijo, "Minimization of Functions Having Lipschitz Continous First partial Derivatives," *Pacific Journal of Mathematics* vol. 16, pp. 1-3, 1966.